

Supplementary Information

Kinetics of protein aggregation at temperature gradient condition

Prasoon Awasthi, Soumen Das*

BioMEMS Laboratory, School of Medical Science and Technology, IIT Kharagpur, India, 721302

*Email-id: sou@smst.iitkgp.ac.in

S1. Nondimensionalisation

$$\frac{\partial c}{\partial t} = D\nabla^2 c + D_T c \nabla^2 T + D_T \nabla c \nabla T \quad (\text{S1})$$

The rescaled variables are defined as following:

$$c' = \frac{c}{c_o}, \quad T' = \frac{T}{T_o}, \quad x' = \frac{x}{L}, \quad \text{and} \quad t' = \frac{t}{\tau}$$

where c_o is monomer concentration at $t = 0$, T_o is the room temperature, L is the solution height, and $\tau = \frac{L^2}{D}$.

The differential operators will be following after applying chain rule:

$$\begin{aligned} \frac{\partial}{\partial t} &= \frac{\partial}{\partial t'} \frac{\partial t'}{\partial t} = \frac{\partial}{\partial t'} \frac{1}{\tau} = \frac{1}{\tau} \frac{\partial}{\partial t'} \\ \frac{\partial}{\partial x} &= \frac{\partial}{\partial x'} \frac{\partial x'}{\partial x} = \frac{\partial}{\partial x'} \frac{1}{L} = \frac{1}{L} \frac{\partial}{\partial x'} \\ \frac{\partial^2}{\partial x^2} &= \frac{\partial}{\partial x} \frac{\partial}{\partial x} = \frac{1}{L} \frac{\partial}{\partial x'} \frac{1}{L} \frac{\partial}{\partial x'} = \frac{1}{L^2} \frac{\partial^2}{\partial x'^2} \end{aligned}$$

Using the above differential operators, the equation S1 becomes as follows:

$$\begin{aligned} \frac{1}{\tau} \frac{\partial (c_o c')}{\partial t'} &= \frac{D}{L^2} \frac{\partial^2 (c_o c')}{\partial x'^2} + \frac{D_T (c_o c')}{L^2} \frac{\partial^2 (T_o T')}{\partial x'^2} + D_T \frac{\partial (c_o c')}{L \partial x'} \frac{\partial (T_o T')}{L \partial x'} \\ \frac{\partial c'}{\partial t'} &= \frac{\partial^2 c'}{\partial x'^2} + \frac{D_T T_o}{D} c' \frac{\partial^2 T'}{\partial x'^2} + \frac{D_T T_o}{D} \frac{\partial c'}{\partial x'} \frac{\partial T'}{\partial x'} \\ \frac{\partial c'}{\partial t'} &= \frac{\partial^2 c'}{\partial x'^2} + S_T T_o \left(\frac{c' \partial^2 T'}{\partial x'^2} + \frac{\partial c'}{\partial x'} \frac{\partial T'}{\partial x'} \right) \end{aligned}$$

where, $S_T = D_T/D$ is the Soret coefficient.

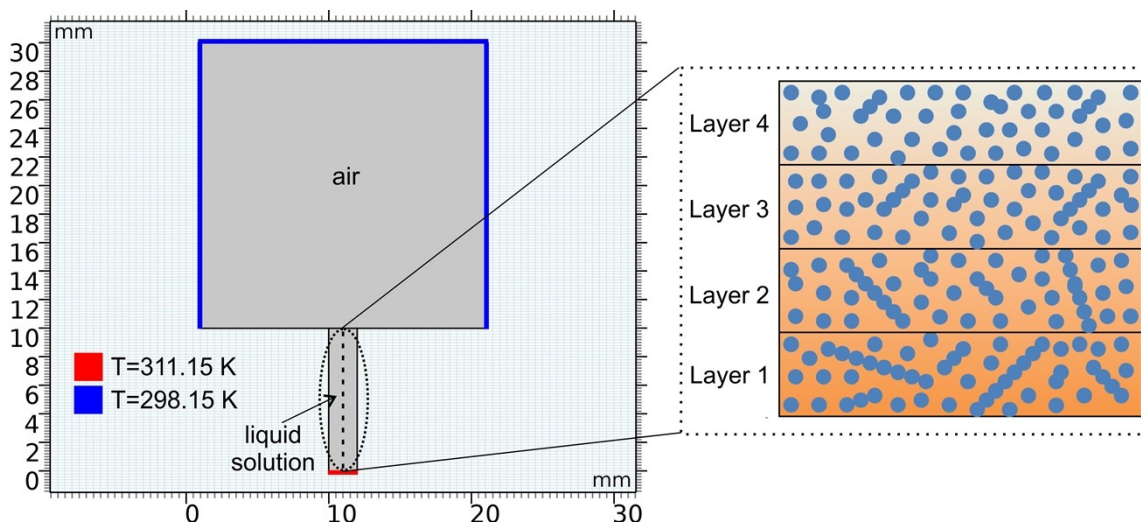


Figure S1: This geometry is used for solving the temperature profile evolution with time. The locations of boundary conditions are shown in red and blue color at 311.15 K and 298.15 K temperature respectively. The whole system is initially at 298.15 K temperature (inset is showing the portion of aqueous solution with four hypothetical layers and the background color gradient demonstrates the steady state temperature profile).

Table S1: This table includes the diffusion constant of monomers and oligomers, and the calculated parameters used to obtain the concentration profiles.

Parameters	Values
Diffusion coefficient of monomers ¹	$1.8 \cdot 10^{-6} \text{ cm}^2/\text{s}$
Diffusion coefficient of oligomers [†]	$0.365 \cdot 10^{-6} \text{ cm}^2/\text{s}$
Thermodiffusion coefficient (D_T) ²	$1.06 \cdot 10^{-8} \text{ cm}^2/\text{s/K}$
Soret coefficient for monomer (calculated)	0.00589 K^{-1}
Soret coefficient for oligomer (calculated)	0.029 K^{-1}
Liquid solution height (L)	1 cm
τ for monomer (calculated)	154.32 h
τ for oligomer (calculated)	761.04 h

[†] It is calculated using Stokes-Einstein relation: $D_O = kT/6\pi\eta R_h$, where D_O , k , T , η , and R_h are diffusion coefficient of oligomer, Boltzmann constant, temperature, solvent viscosity, and hydrodynamic radius of oligomer respectively. The viscosity of water at 37°C is 0.6913 mPa.s, and R_h of 9 nm is chosen for oligomer. Different oligomeric species in dynamic equilibrium ³⁻⁵ create their concentration gradient along the y-axis depending on their hydrodynamic radius. We only choose hydrodynamic radius of 9 nm from the literature ^{6,7} for its concentration profile instead of many sizes to avoid redundancy in the plot. Because if we take higher hydrodynamic radius of oligomer, we will even obtain the slower change in the average concentration of oligomer as compared to oligomer of 9 nm hydrodynamic radius due to decreased diffusion coefficient leading us to the same conclusion.

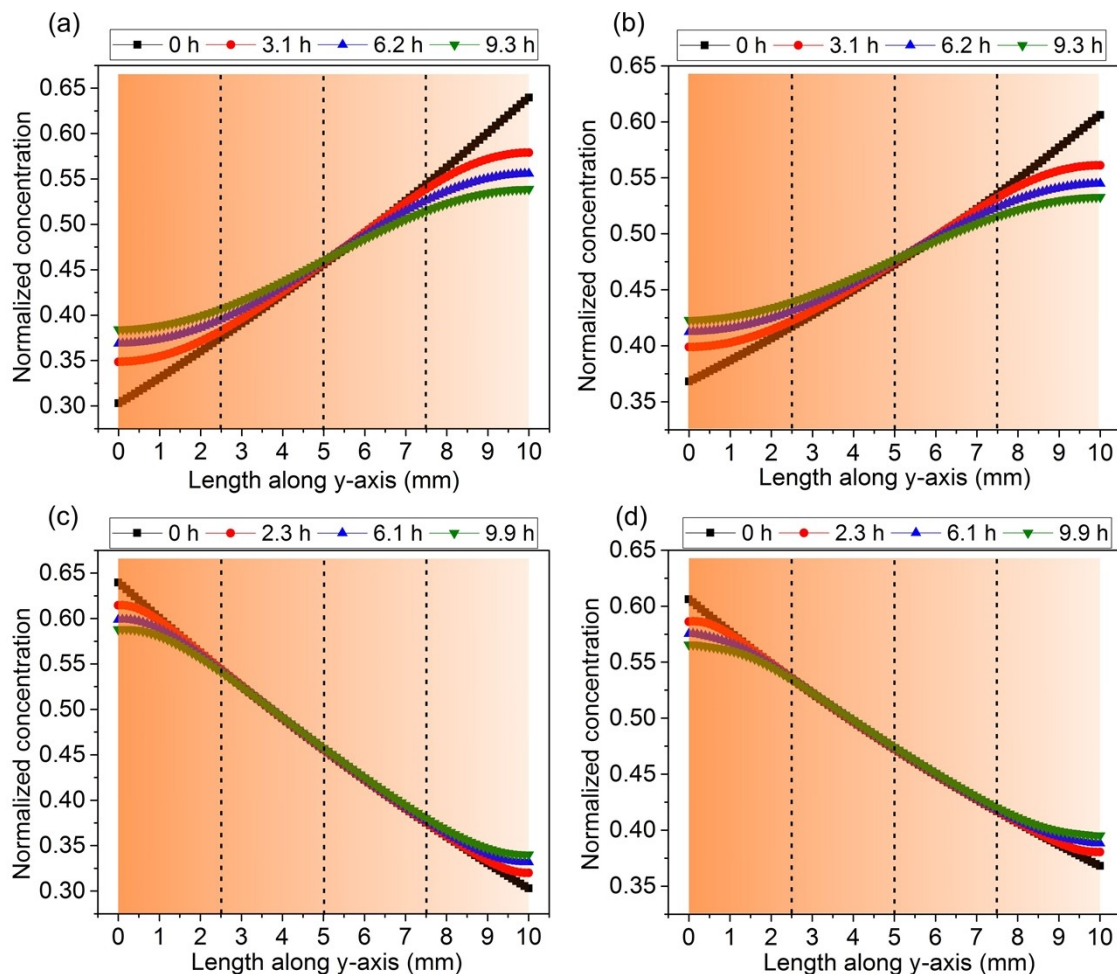


Figure S2: Change in normalized concentration profile of monomers: (a) for parabolic $(0.55+y/4)^2$, (b) for exponential $(e^{(y/2)-1})$ initial conditions, and oligomers: (c) for parabolic $(0.8-y/4)^2$ (d) for exponential $(e^{-(y+1)/2})$ initial conditions, along y-axis of solution with time.

S2. Justification for solving the protein aggregation kinetic equations independently in the four layers

To demonstrate the effect of change in average normalized concentration of monomer in the hypothetical layer on protein aggregation kinetics, we numerically solve the kinetic equations (5)-(7) including this change in the concentration. The values of average normalized concentration of monomer in each hypothetical layer for the Fig 2(ii) are listed in Table S2. It is observed that the monomer concentration is increasing in the layer 1 and reducing in layer 4. So, the kinetic equations for layer 1 and 4 are solved with incoming and outgoing flux of monomers respectively, and the parameters' value are kept similar for layer 1 and 4 as listed in Table 1. Figure S3(a) and (b) are showing the mass concentration profile for layer 1 and 4 respectively. It is observed that there is no significant impact on the protein aggregation kinetics in the layers.

Table S2: Average normalized concentration of monomers in the hypothetical layers with time

Time	0 h	3.1 h	6.2 h	9.3 h
Layer 1	0.375	0.399	0.417	0.432
Layer 2	0.460	0.462	0.467	0.473
Layer 3	0.543	0.541	0.535	0.529
Layer 4	0.627	0.602	0.583	0.569

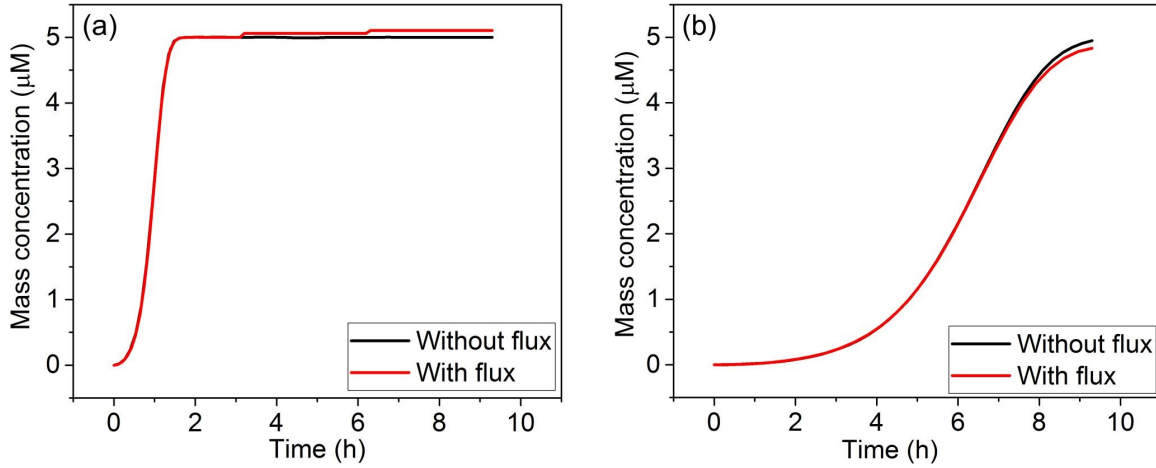


Figure S3: (a) and (b) show the mass concentration profile for without flux and with flux of monomer using layer 1 and 4 parameters' value respectively.

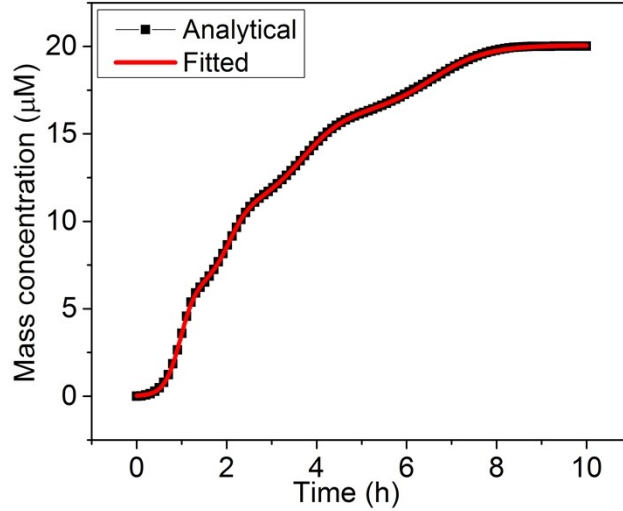


Figure S4: Fitting the analytical multi-sigmoidal graph with $y = y_0 + \sum_{i=1}^4 y_i / [1 + e^{-(t-t_{1/2})/\tau_{E_i}}]$.

Table S3: Obtained parameters from fitting plot shown in Figure S3 (standard error is fitting error)

Layer	$t_{1/2}$ (value \pm SE)	τ_{E_i} (value \pm SE)
1	58.15 \pm 0.26 min	10.50 \pm 0.15 min
2	123.23 \pm 0.48 min	13.62 \pm 0.53 min

3	221.08 ± 0.98 min	28.70 ± 0.93 min
4	395.19 ± 1.13 min	35.61 ± 0.73 min

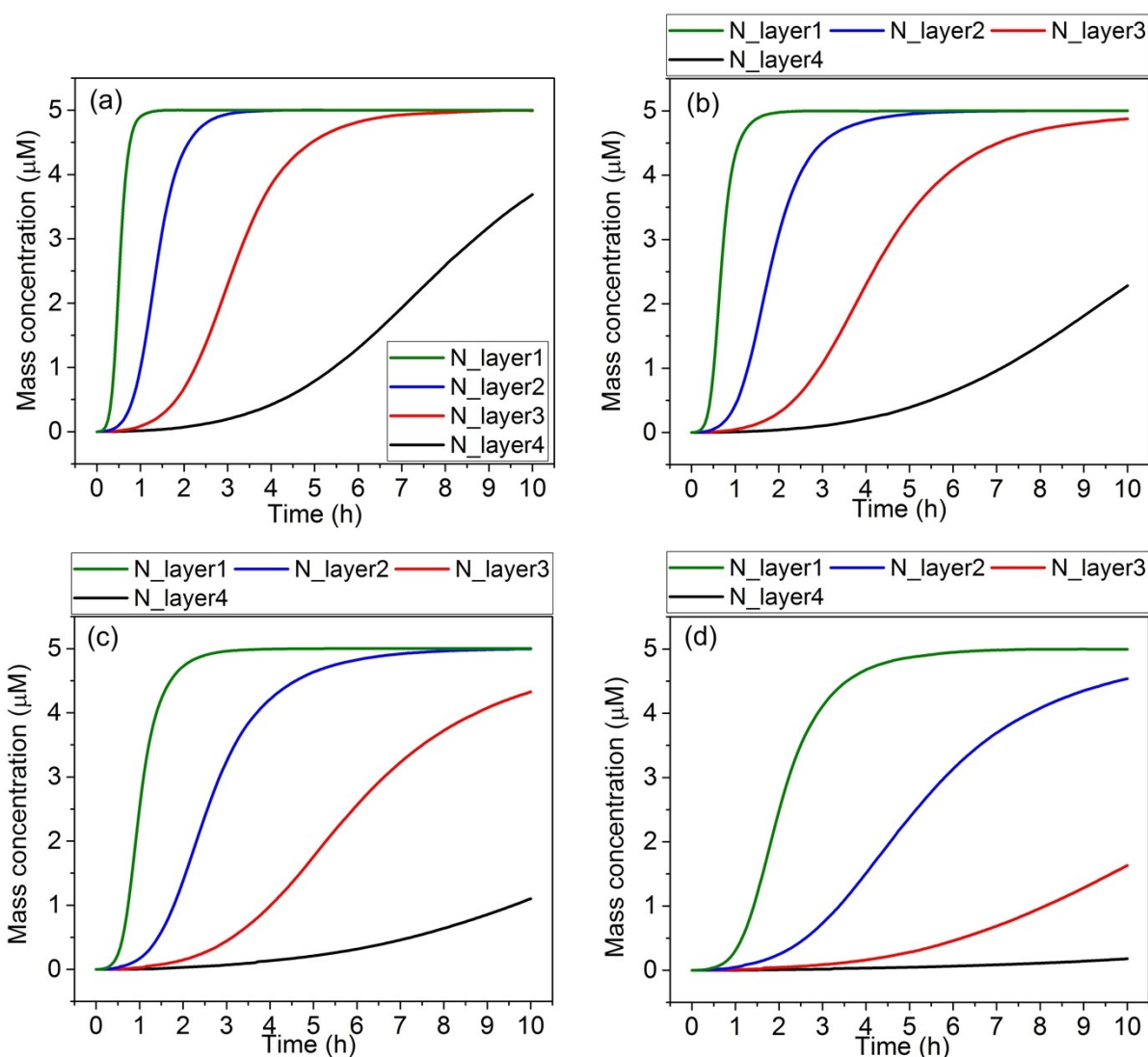


Figure S5. (a), (b), (c), (d), and (e) are the time evolution of fibril mass concentration at the four layers in the presence of inhibitor at the concentration of 1 μM , 5 μM , 10 μM , and 20 μM respectively. (N represents the numerical solution)

References:

- 1 J. Waters, *PLoS One*, 2010, **5**, e15709.
- 2 M. Fränzl, T. Thalheim, J. Adler, D. Huster, J. Posseckardt, M. Mertig and F. Cichos, *Nat. Methods*, 2019, **16**, 611–614.
- 3 D. M. Walsh and D. J. Selkoe, *J. Neurochem.*, 2007, **101**, 1172–1184.
- 4 J. J. Mittag, S. Milani, D. M. Walsh, J. O. Rädler and J. J. McManus, *Biochem. Biophys. Res. Commun.*,

- 2014, **448**, 195–199.
- 5 E. Hellstrand, B. Boland, D. M. Walsh and S. Linse, *ACS Chem. Neurosci.*, 2009, **1**, 13–18.
- 6 S. S.-S. Wang, A. Becerra-Arteaga and T. A. Good, *Biotechnol. Bioeng.*, 2002, **80**, 50–59.
- 7 N. E. Pryor, M. A. Moss and C. N. Hestekin, *Int. J. Mol. Sci.* 2012, Vol. 13, Pages 3038-3072, 2012, **13**, 3038–3072.